Featured in Physics

Circumventing Magnetostatic Reciprocity: A Diode for Magnetic Fields

J. Prat-Camps,[1,2,3,*] P. Maurer,[1,2] G. Kirchmair,[1,4] and O. Romero-Isart[1,2]
[1]Institute for Quantum Optics and Quantum Information of the Austrian Academy of Sciences, A-6020 Innsbruck, Austria
[2]Institute for Theoretical Physics, University of Innsbruck, A-6020 Innsbruck, Austria
[3]INTERACT Lab, School of Engineering and Informatics, University of Sussex, Brighton BN1 9RH, United Kingdom
[4]Institute for Experimental Physics, University of Innsbruck, A-6020 Innsbruck, Austria

(Received 15 May 2018; published 20 November 2018)

Lorentz reciprocity establishes a stringent relation between electromagnetic fields and their sources. For static magnetic fields, a relation between magnetic sources and fields can be drawn in analogy to the Green's reciprocity principle for electrostatics. So far, the magnetostatic reciprocity principle remains unchallenged and the magnetostatic interaction is assumed to be symmetric (reciprocal). Here, we theoretically and experimentally show that a linear and isotropic electrically conductive material moving with constant velocity is able to circumvent the magnetostatic reciprocity principle and realize a diode for magnetic fields. This result is demonstrated by measuring an extremely asymmetric magnetic coupling between two coils that are located near a moving conductor. The possibility to generate controlled unidirectional magnetic couplings implies that the mutual inductances between magnetic elements or circuits can be made extremely asymmetric. We anticipate that this result will provide novel possibilities for applications and technologies based on magnetically coupled elements and might open fundamentally new avenues in artificial magnetic spin systems.

DOI: 10.1103/PhysRevLett.121.213903

Lorentz reciprocity is a general principle that relates electromagnetic (EM) fields with their sources. Arising directly from Maxwell equations, it has a fundamental importance in a huge variety of EM systems and technologies, ranging from radio-wave and microwave antennas to photonic communication systems, to name only a few. Finding ways to break the Lorentz reciprocity principle has raised a lot of interest lately [1,2], since it is a necessary condition to build true EM isolators that allow the propagation of signals in one direction while preventing backaction in the opposite one [3]. Recently, it has been shown that breaking Lorentz reciprocity also allows us to overcome fundamental time-bandwidth limitations in resonant systems [4]. The concept of reciprocity extends to other physical systems, like acoustic wave propagation or mechanical systems [5–7]. Also there, one aims at breaking reciprocity to achieve one-way signal propagation. In the context of microwaves and photonic systems, the magneto-optical effect (Faraday rotation) has been traditionally used to break reciprocity. However, such an effect relies on the application of an external magnetic bias, which makes it unsuitable for on-chip miniaturization and integration. This has prompted the development of a whole new generation of magnetic-free nonreciprocal devices mainly based on the application of other bias vectors which are odd under time reversal. This includes the spatiotemporal modulation of material properties to impart angular momentum bias [8–11], linear momentum [12], or commutation [13]. It has been realized that optomechanical coupling can also be used to induce electromagnetic nonreciprocity [14], see [15] and references therein.

In the static limit, Maxwell equations decouple and reciprocity needs to be revised. In electrostatics, Green's reciprocity [16,17] relates two independent charge distributions, ρ_1 and ρ_2, with their corresponding electrostatic potentials, V_1 and V_2, via $\int d\mathbf{r}\rho_1 V_2 = \int d\mathbf{r}\rho_2 V_1$. For the magnetostatic case, one can do an analogous derivation. Consider two independent distributions of current densities, $\mathbf{J}_1$ and $\mathbf{J}_2$, that create the magnetic fields $\mathbf{H}_1$ and $\mathbf{H}_2$, respectively. The corresponding magnetic vector potentials, $\mathbf{A}_1$ and $\mathbf{A}_2$, are related to the fields through the magnetic permeability tensor, $\bar{\bar{\mu}}$, as $\bar{\bar{\mu}}\mathbf{H}_i = \nabla \times \mathbf{A}_i$ $(i = 1, 2)$. Using the two sets of magnetostatic Maxwell equations and manipulating them, one finds $\nabla \cdot (\mathbf{H}_1 \times \mathbf{A}_2 - \mathbf{H}_2 \times \mathbf{A}_1) = \mathbf{H}_2\bar{\bar{\mu}}\mathbf{H}_1 - \mathbf{H}_1\bar{\bar{\mu}}\mathbf{H}_2 + \mathbf{A}_2 \cdot \mathbf{J}_1 - \mathbf{A}_1 \cdot \mathbf{J}_2$ (see Supplemental Material [18]). The first two terms cancel out if (i) permeability is a symmetric tensor, $\bar{\bar{\mu}} = \bar{\bar{\mu}}^{\mathrm{T}}$, and (ii) $\bar{\bar{\mu}}$ is linear (i.e., does not depend on the magnetic field). By integrating over all space, the left-hand side vanishes. This leads to the reciprocity condition for magnetostatic fields, [25]

$$\int d\mathbf{r}\mathbf{A}_2 \cdot \mathbf{J}_1 = \int d\mathbf{r}\mathbf{A}_1 \cdot \mathbf{J}_2. \tag{1}$$

This expression reads similar to the Lorentz reciprocity equation for electromagnetic waves and localized sources, $\int d\mathbf{r}\mathbf{E}_2 \cdot \mathbf{J}_1 = \int d\mathbf{r}\mathbf{E}_1 \cdot \mathbf{J}_2$ [1,4], with $\mathbf{E}$ being the electric field. As shown in the Supplemental Material [18], though,

the derivation of the Lorentz reciprocity condition assumes coupled electric and magnetic fields and, thus, one cannot make the zero-frequency limit directly. At the same time, static conditions (no temporal variation of fields, sources or material properties) impose severe constrains when one aims at circumventing magnetostatic reciprocity; there is no magneto-optical coupling and temporal modulation of the material properties is not compatible with static conditions [26].

The magnetostatic reciprocity condition in Eq. (1) can be rewritten in different ways. When sources are point magnetic dipoles with moments $\mathbf{m}_1$ and $\mathbf{m}_2$, located at positions $\mathbf{r}_1$ and $\mathbf{r}_2$, respectively, it simplifies to $\mathbf{B}_2(\mathbf{r}_1)\cdot\mathbf{m}_1 = \mathbf{B}_1(\mathbf{r}_2)\cdot\mathbf{m}_2$, where $\mathbf{B}_i$ is the magnetic induction field created by the ith dipole. Alternatively, when sources are closed magnetic circuits, Eq. (1) becomes $M_{12} = M_{21}$, with M_{nm} being the mutual inductance between the nth and the mth circuits. This shows how the magnetic reciprocity principle is responsible for the symmetry of magnetic couplings [27,28].

The magnetostatic reciprocity principle formulated in Eq. (1) holds for linear materials with locally symmetric permeability tensors [$\bar{\bar{\mu}}(\mathbf{r}) = \bar{\bar{\mu}}(\mathbf{r})^{\mathrm{T}}$]. This includes magnetic metamaterials [29–36] which, despite of being complex arrangements of different magnetic materials with unusual effective magnetic properties, are locally symmetric. Hence, magnetic metamaterials cannot break the magnetic reciprocity principle even in extremely counterintuitive cases, see [18].

Let us now show how, in spite of using linear, isotropic, and homogeneous materials one can optimally circumvent the magnetic reciprocity principle by means of a moving electrical conductor. When a conductor with electrical conductivity σ moves with velocity $v \ll c$ (c is the speed of light) in the presence of a magnetic field, a current density given by $\mathbf{J}_{\mathrm{mc}} = \sigma\mathbf{v}\times\mathbf{B}$ is induced [37]. If one includes this term in the previous reciprocity derivation, an extra factor appears reading $\sigma\mathbf{v}\cdot[(\nabla\times\mathbf{A}_1)\times\mathbf{A}_2 - (\nabla\times\mathbf{A}_2)\times\mathbf{A}_1]$. This factor, generally different from zero, shows how a moving conductor can break reciprocity.

As a particular case, we consider a semi-infinite conductor that extends to $z < 0$. We assume it has a constant electrical conductivity σ and a velocity $\mathbf{v} = v\hat{e}_x$. We evaluate the magnetic reciprocity between two identical dipoles, $\mathbf{m}_1 = \mathbf{m}_2 = m\hat{e}_j$ (with $\hat{e}_j$ being a unit vector, $j = x, y, z$) situated at $\mathbf{r}_1 = (-\delta/2, 0, z_0)$ and $\mathbf{r}_2 = (\delta/2, 0, z_0)$, respectively, see Fig. 1 left (δ, $z_0 > 0$). Since the conductor is translationally invariant along x, this problem is equivalent to considering a single magnetic point dipole with moment $\mathbf{m} = m\hat{e}_j$ located at $\mathbf{r} = (0, 0, z_0)$ and evaluating the magnetic field at the positions $\mathbf{r}_+ = (\delta, 0, z_0)$ and $\mathbf{r}_- = (-\delta, 0, z_0)$, see Fig. 1 right. Reciprocity dictates that the *isolation*, defined as $\mathcal{I}_j \equiv B_j(\mathbf{r}_-)/B_j(\mathbf{r}_+)$, is $\mathcal{I}_j = 1$.

We analytically solve the Lorentz-transformed problem of a dipole moving with constant velocity at a fixed height z_0 above a semi-infinite surface characterized by a complex

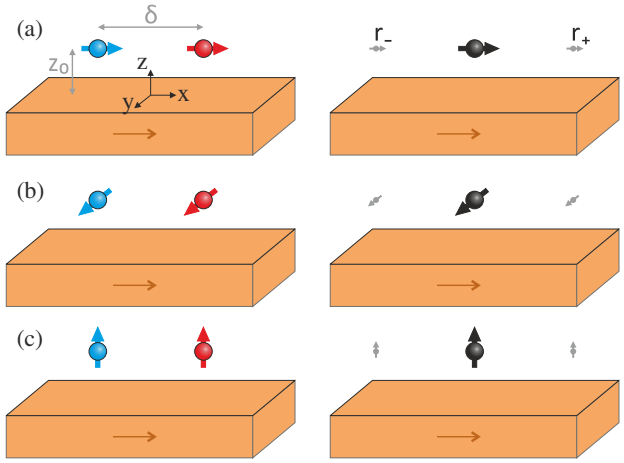

FIG. 1. (Left) Sketch of the magnetic dipoles between which magnetic reciprocity is evaluated ($\mathbf{m}_1$ in blue and $\mathbf{m}_2$ in red). For translationally symmetric systems, this is equivalent to considering a single dipole (right) and evaluating the component of the field parallel to the dipole at $\mathbf{r}_+$ and $\mathbf{r}_-$.

permittivity $\varepsilon(\omega) = 1 + i\sigma/(\varepsilon_0\omega)$ [18]. The scattered field is obtained everywhere in the upper half-space. In general, this field does not show any clear symmetry and strongly depends on the magnetic Reynolds number, $R_m \equiv \mu_0\sigma v z_0$ (with μ_0 being the vacuum permeability). For small Reynolds numbers ($R_m \ll 1$), the scattered field can be approximated to an antisymmetric function of δ. In this case the effect of the conductor is clear; since the field of the bare dipole is symmetric, the moving conductor increases the field on one side but decreases it on the other. The inverse of the isolation between dipoles, arranged in the three different configurations, is plotted in Fig. 2; the curves only depend on δ/z_0 and R_m. These plots show how the moving conductor generates isolations different from 1 and, thus, breaks magnetic reciprocity for the three different dipole orientations. However, while isolations between x-oriented dipoles are small (values near one), y and z orientations result in isolations that go from positive to negative values through a divergence. The existence of δ's for which the isolation is infinite (we refer to the points where $\mathcal{I}_j^{-1} = 0$ as δ_0^j for $j = y, z$) demonstrates that one can achieve a maximally asymmetric (unidirectional) magnetic coupling between the dipoles. For example, for two dipoles oriented along z and located at $\mathbf{r}_1 = (-\delta_0^z/2, 0, z_0)$ and $\mathbf{r}_2 = (\delta_0^z/2, 0, z_0)$, one finds that $B_{z,1}(\mathbf{r}_2) = 0$ while $B_{z,2}(\mathbf{r}_1) \neq 0$. If dipoles are interpreted as small circular coils with axis along the z direction, then this means that the magnetic flux threading coil 1 is different from zero while the flux through coil 2 is zero. Therefore, the mutual inductance between the two magnetic elements becomes maximally asymmetric, with $M_{12} = 0$ and $M_{21} \neq 0$. In this sense, a unidirectional magnetic coupling is achieved, realizing a perfect diode for magnetic fields.

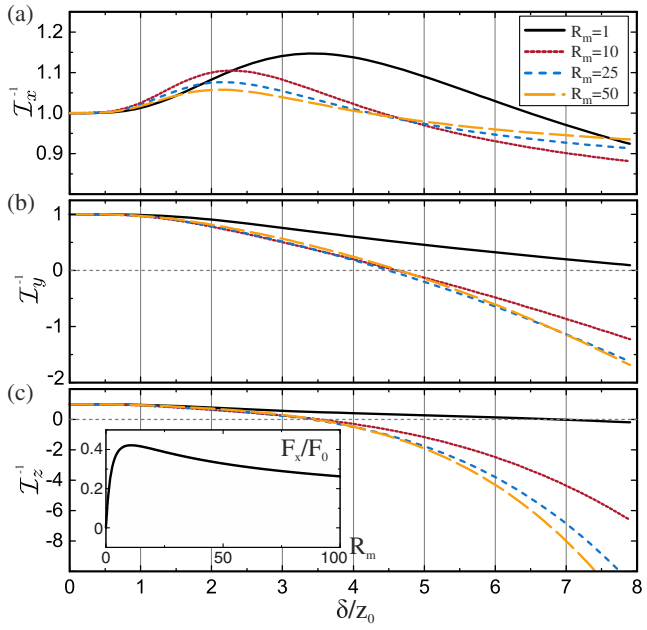

FIG. 2. Plots of the inverse of the isolation as a function of δ/z_0 for dipoles oriented along (a) x, (b) y, and (c) z directions for different values of R_m. Inset in (c) shows the normalized force F_x/F_0 [$F_0 \equiv \mu_0 m^2/(8\pi^2 z_0^4)$] on a z oriented dipole as a function of R_m. Notice that, since the materials involved are linear, these plots (and therefore, the points of infinite isolation) do not depend on the modulus of the magnetic dipole.

Note that this mechanism is intrinsically lossy; one needs to add energy to the system in order to keep the conductor moving at a constant velocity and overcome the magnetic friction originating from the induced eddy currents. The power dissipated by the system of Fig. 1 right is given by $P = -vF_x$, where F_x is the x component of the force acting on the dipole as a result of these currents. The force can be analytically calculated from the field scattered by the conductor [18]. As shown in the inset of Fig. 2(c), the normalized force only depends on R_m and has a nonmonotonic behavior; it is 0 for $R_m = 0$ (when the conductor is at rest), grows linearly for small R_m, reaches a maximum value for $R_m \approx 10$, and decreases as $R^{-1/2}$ for $R_m \gg 10$. This force has a similar velocity dependence as the vacuum frictional force between two conducting surfaces [38], which is maximal for a certain velocity and monotonically decreases for bigger values. Interestingly, it can be demonstrated that for a perfect electric conductor ($\varepsilon \to \infty$), reciprocity is preserved and $\mathcal{I} = 1$ for all δ. In this ideal case the system is lossless and the dipole experiences no force. For consistency, we also checked that the Lorentz-transformed problem with the dipole at rest and the conductor moving with constant velocity leads to the same results. We solved this problem numerically with COMSOL MULTIPHYSICS by introducing a free current density $\mathbf{J}_{\mathrm{mc}}$ in the conductor, finding good agreement with our analytical results.

Finally, we remark that these results are also valid for low-frequency oscillating magnetic fields. We analytically solve the problem of a z-oriented magnetic dipole, whose moment oscillates as $\mathbf{m}(t) = m\cos(\omega_0 t)\hat{e}_z$. For $\omega_0 \ll |v/z_0|$, one finds that the magnetic field distribution is the same as for the static case, simply modulated by a $\cos(\omega_0 t)$ function [18]. Therefore, even for low-frequency oscillating magnetic sources and circuits, the moving conductor is able to generate a maximally asymmetric magnetic coupling between them.

We shall now present the experimental demonstration of these results. Our setup consists of a circularly symmetric conductor with a U-shaped cross section, as sketched in Fig. 3(a), that moves with constant angular velocity around its axial symmetry axis. The previous analysis indicates that the magnetic moment of the dipole has to be perpendicular to the velocity in order to generate points of infinite isolation. For this reason, we put a small coil inside the moving conductor space, with its axis pointing along the radial direction. A second coil is placed at a given distance with analogous radial orientation, and the magnetic coupling between them is measured [18]. For experimental convenience, the experiment is performed with low-frequency oscillating magnetic fields. We use a signal generator to feed the first coil, while the voltage induced in the second (pickup) coil is measured through a lock-in amplifier. Lock-in measurements provide a good signal-to-noise ratio even for small magnetic fields and allow us to get rid of slowly fluctuating magnetic fields in the environment. At the low frequencies we consider, the coupling between magnetic and induced electric field is negligible and, thus, these measurements effectively describe the static case. Measurements of the out-of-phase voltage for a signal frequency of $\omega_0/(2\pi) = 9$ Hz are shown in Fig. 3(c), as a function of the rotation frequency of the conductor, ν. Measurements are repeated for three different positions of the pickup coil (see inset). For positive rotation frequencies, the measured voltage decreases and crosses 0 for positions r_2 and r_3 of the pickup coil. At position r_1, the field scattered by the conductor is not able to fully cancel the field of the source for the velocities we considered. When moving in the opposite direction, the conductor increases the measured voltage. These measurements convincingly demonstrate that magnetic reciprocity is broken and that points of infinite isolation (for which the measured voltage is zero for positive rotation frequency but different from zero for negative) are generated by means of a moving conductor. These zero-voltage points are found in spite of the extended size of the pickup coil; the field goes from positive to negative values around the zero and thus, the total magnetic flux threading the coil cancels out at some point. As can be seen, the error bars associated with our measurements are very small compared to the measured voltages. These errors come from the measured voltage fluctuations over time (plotted error bars correspond to 1σ).

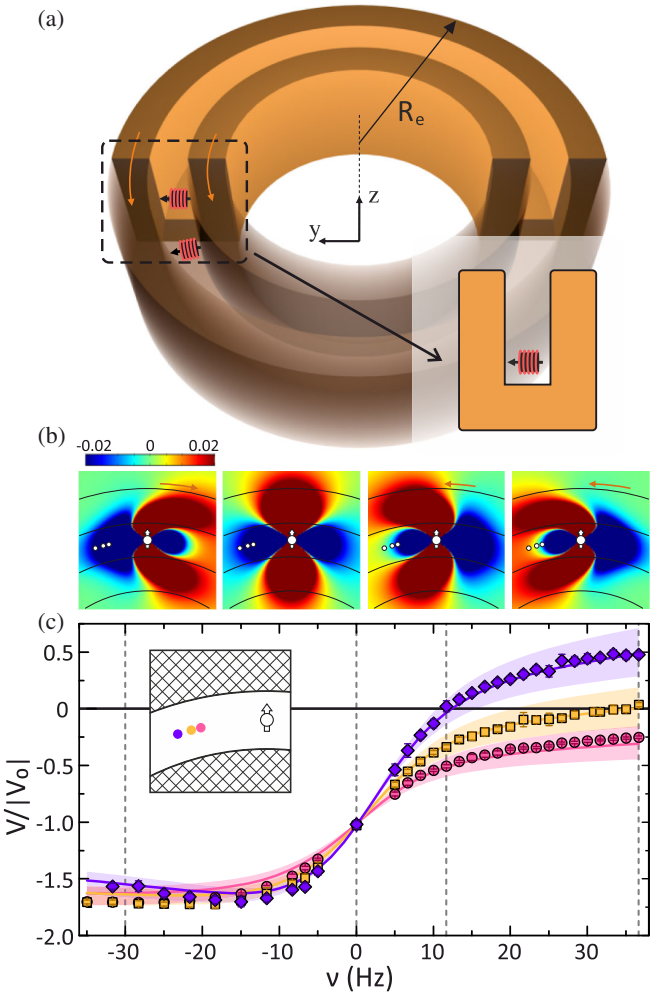

FIG. 3. (a) Sketch of the experimental setup; a circular U-shaped conductor (orange, with $R_e = 65$ mm) moves with rotation frequency ν around the z axis (arrows indicate the positive rotation direction). Two coils (in red), whose axes are radially aligned, are used to measure the magnetic coupling between them. (b) Numerical calculations for an oscillating magnetic dipole [in white, for $\omega_0/(2\pi) = 9$ Hz]. Colors correspond to the real part of the normalized radial field, B_ρ/B_0 [where $B_0 \equiv \mu_0 m/(2\pi z_0^3)$ with $z_0 = 5$ mm] for different rotation frequencies of the conductor, $\nu = -30$, 0, 11.7, and 36.7 Hz (from left to right). Plots show the magnetic field distribution evaluated at the plane of the dipole. White dots indicate positions where measurements were taken. (c) Out-of-phase component of the voltage measured in the receiving coil (symbols) as a function of the velocity of the conductor [for a signal frequency of $\omega_0/(2\pi) = 9$ Hz]. Measurements were taken at three different distances from the source coil, $r_1 = 11.4$ mm (pink), $r_2 = 13.1$ mm (yellow), and $r_3 = 15.5$ mm (purple), see inset. For each distance, measurements are normalized to the voltage induced at the receiving coil in free space, $|V_0|$. Solid lines are the corresponding numerical calculations considering point dipoles. Shadow areas are defined by considering uncertainties in the experimental parameters used for the numerical calculations [18]. Dashed vertical lines indicate the frequencies of the numerical calculations in (b). Error bars (1σ) are shown for the three cases; most of them are symbol size or smaller.

All these measurements agree very well with the corresponding 3D numerical calculations [solid lines in Fig. 3(c)] considering the coils as point dipoles. The main source of uncertainty between our measurements and the numerical calculations comes from the positioning of the coils relative to each other and to the moving conductor. We tried to estimate the effects of imprecise positioning by running different numerical calculations in which we changed the distance between the coils (± 0.5 mm) and their relative position with respect to the conductor (± 0.5 mm in the z direction). The results were used to create the shadow bands in Fig. 3(c), defined as the result with the largest deviation for each ν from the nominal calculation. Numerical calculations also provide a deeper understanding on how the conductor shapes the distribution of magnetic field. In Fig. 3(b), we show numerical calculations of the real part of the B_ρ field (being B_ρ the radial component of the field in cylindrical coordinates, $\rho = \sqrt{x^2 + y^2}$) created by a magnetic dipole (in white) oscillating at a frequency $\omega_0/(2\pi) = 9$ Hz. The symmetric field distribution when the conductor is at rest (second panel) becomes clearly asymmetric as it moves in one direction (first panel). When moving in the opposite direction (third and fourth panels), the field distribution flips direction. This evidences the existence of points of infinite isolation (points of zero field, in green color).

Measurements were repeated for higher signal frequencies [18]. In all cases the agreement with the corresponding numerical calculations is excellent. Finally, we measure the actual mutual inductance between the two coils to demonstrate how extremely asymmetric values are achieved. The second coil is placed at r_2 and is connected to the lock-in amplifier, while the first coil is connected to the signal generator. With the conductor at rest ($\nu = 0$), we measure $M_{12} = (22 + 3i)$ nH. We then exchange the connections to the coils and measure the opposite coupling, finding a symmetric mutual inductance, $M_{21} = M_{12}$, in agreement with the magnetic reciprocity principle. This same procedure is repeated with the conductor moving at $\nu = 33.3$ Hz. In this case, we first measure $M'_{12} = (0 + 2i)$ nH and, after exchanging the connections, we find $M'_{21} = (36 + 0i)$ nH [39] (both measurements have an error of ± 0.6 nH [18]). These measurements demonstrate how, by tuning the velocity of the conductor, the magnetic coupling between the coils becomes unidirectional.

The use of a moving conductive material to break magnetic reciprocity boils down to the Lorentz force that the free electrons of the conductor experience as they move through the magnetic field. In principle, one could replace the mechanical movement of the whole material by an externally applied electric field, which would force the electrons to move with a constant mean velocity in the conductor according to Ohm's law. While theoretically correct, this approach is limited by the small mean velocity at which electrons move in metals for reasonable current

densities. For copper, e.g., the standard maximum current density of 500 A/cm^2 corresponds to mean velocities $\sim 4 \times 10^{-4}$ m/s, in contrast to the linear velocities achieved in our setup of ~ 3.1 m/s for $\nu = 10$ Hz (see [18] for a detailed discussion using the Drude model). Interestingly, other materials like graphene exhibit carrier mobilities that can be more than 3 orders of magnitude larger than in copper [40] while being able to sustain current densities on the order of $\sim 10^8$ A/cm^2 [41]. Hence, graphene is an interesting candidate to explore implementations that do not rely on mechanical movement of macroscopic objects.

In conclusion, we have demonstrated that the magnetostatic reciprocity principle can be circumvented by means of a linear and isotropic electrical conductor moving with constant velocity. The nonreciprocal response of the system is controlled trough the velocity of the conductor, making it possible to achieve an infinite magnetic isolation (i.e., a perfectly unidirectional magnetic coupling) and to realize a diode for magnetic fields. The concept, which relies only on linear materials and low (nonrelativistic) velocities, may open the door to novel possibilities for a large number of systems and technologies that employ magnetically coupled elements. In particular, the breaking of magnetostatic reciprocity could be useful to increase the efficiency of magnetically based wireless power transfer technologies. This would allow the energy to flow from the emitting to the receiving circuit but would prevent the flow in the opposite direction. Other key technologies based on magnetically coupled circuits, like transformers, could also benefit from this same principle. Results presented here could also open new horizons in fundamental research areas, like artificial magnetic spin systems. A conductor moving near a system of artificial spins would alter the reciprocal dipole-dipole interaction between them, potentially forcing the system to crystallize in nonconventional structures.

This work is supported by the European Research Council (ERC-2013-StG 335489 QSuperMag) and the Austrian Federal Ministry of Science, Research, and Economy (BMWFW). J. P. C. acknowledges discussions with the Superconductivity Group of the Universitat Autonoma de Barcelona. We acknowledge the help of S. Oleschko and our in-house workshop for the fabrication of the experimental setup.

*j.prat.camps@gmail.com

[1] R. J. Potton, Rep. Prog. Phys. **67**, 717 (2004).
[2] C. Caloz, A. Alù, S. Tretyakov, D. Sounas, K. Achouri, and Z.-L. Deck-Léger, Phys. Rev. Applied **10**, 047001 (2018).
[3] D. Jalas *et al.*, Nat. Photonics **7**, 579 (2013).
[4] K. L. Tsakmakidis, L. Shen, S. A. Schulz, X. Zheng, J. Upham, X. Deng, H. Altug, A. F. Vakakis, and R. W. Boyd, Science **356**, 1260 (2017).
[5] R. Fleury, D. L. Sounas, C. F. Sieck, M. R. Haberman, and A. Alù, Science **343**, 516 (2014).
[6] S. A. Cummer, J. Christensen, and A. Alù, Nat. Rev. Mater. **1**, 16001 (2016).
[7] C. Coulais, D. Sounas, and A. Alù, Nature (London) **542**, 461 (2017).
[8] D. L. Sounas, C. Caloz, and A. Alù, Nat. Commun. **4**, 2407 (2013).
[9] N. A. Estep, D. L. Sounas, J. Soric, and A. Alù, Nat. Phys. **10**, 923 (2014).
[10] A. Kamal, J. Clarke, and M. H. Devoret, Nat. Phys. **7**, 311 (2011).
[11] D. L. Sounas and A. Alù, Nat. Photonics **11**, 774 (2017).
[12] S. Qin, Q. Xu, and Y. E. Wang, IEEE Trans. Microwave Theory Tech. **62**, 2260 (2014).
[13] N. Reiskarimian and H. Krishnaswamy, Nat. Commun. **7**, 11217 (2016).
[14] S. Manipatruni, J. T. Robinson, and M. Lipson, Phys. Rev. Lett. **102**, 213903 (2009).
[15] M.-A. Miri, F. Ruesink, E. Verhagen, and A. Alù, Phys. Rev. Applied **7**, 064014 (2017).
[16] J. D. Jackson, *Classical Electrodynamics*, 3rd ed. (Wiley, New York, 1999).
[17] D. J. Griffiths, *Introduction to Electrodynamics*, 3rd ed. (Prentice Hall, New Jersey, 1999).
[18] See Supplemental Material at http://link.aps.org/supplemental/10.1103/PhysRevLett.121.213903 for further analytical derivations, experimental details, and measurements at other signal frequencies, which includes Refs. [19–24].
[19] R. Carminati, M. Nieto-Vesperinas, and J.-J. Greffet, J. Opt. Soc. Am. A **15**, 706 (1998).
[20] J. M. D. Coey, *Magnetism and Magnetic Materials* (Cambridge University Press, Cambridge, England, 2010).
[21] A. L. Kholmetskii, O. V. Missevitch, and T. Yarman, Eur. Phys. J. Plus **131**, 316 (2016).
[22] S. Y. Buhmann, *Dispersion Forces I* (Springer-Verlag, Berlin, 2012).
[23] A. Thess, E. Votyakov, B. Knaepen, and O. Zikanov, New J. Phys. **9**, 299 (2007).
[24] N. W. Ashcroft and N. D. Mermin, *Solid State Physics* (Saunders, Philadelphia, 1976).
[25] A. Zangwill, *Modern Electrodynamics* (Cambridge University Press, Cambridge, England, 2013).
[26] This means that none of the electromagnetic material properties (electric permittivity, magnetic permeability, or electrical conductivity) can change over time, i.e., none of these properties can have any explicit dependence on time.
[27] F. M. Tesche, M. Ianoz, and T. Karlsson, *EMC Analysis Methods and Computational Models* (Wiley, New York, 1997).
[28] L. O. Chua, C. A. Desoer, and E. S. Kuh, *Linear and Nonlinear Circuits* (McGraw-Hill, New York, 1987).
[29] B. Wood and J. B. Pendry, J. Phys. Condens. Matter **19**, 076208 (2007).
[30] F. Magnus, B. Wood, J. Moore, K. Morrison, G. Perkins, J. Fyson, M. C. K. Wiltshire, D. Caplin, L. F. Cohen, and J. B. Pendry, Nat. Mater. **7**, 295 (2008).
[31] S. M. Anlage, J. Opt. **13**, 024001 (2011).

[32] A. Sanchez, C. Navau, J. Prat-Camps, and D.-X. Chen, New J. Phys. **13**, 093034 (2011).
[33] S. Narayana and Y. Sato, Adv. Mater. **24**, 71 (2012).
[34] R. Wang, Z. L. Mei, and T. J. Cui, Appl. Phys. Lett. **102**, 213501 (2013).
[35] J. Prat-Camps, C. Navau, and A. Sanchez, Appl. Phys. Lett. **105**, 234101 (2014).
[36] J. Prat-Camps, C. Navau, and A. Sanchez, Adv. Mater. **28**, 4898 (2016).
[37] L. D. Landau and E. M. Lifshitz, *Electrodynamics of Continuous Media* (Pergamon, Oxford, 1960), Vol. 8.
[38] J. B. Pendry, J. Phys. Condens. Matter **9**, 10301 (1997).
[39] In all these measurements the imaginary part of the mutual inductance results from the eddy-current losses in the conductor due to the fact that measurements are done at a finite frequency (9 Hz). In the strict static case, inductances would be purely real.
[40] J.-H. Chen, C. Jang, S. Xiao, M. Ishigami, and M. S. Fuhrer, Nat. Nanotechnol. **3**, 206 (2008).
[41] R. Muralia, Y. Yang, K. Brenner, T. Beck, and J. D. Meindl, Appl. Phys. Lett. **94**, 243114 (2009).